A TRIDENT SCHOLAR PROJECT REPORT

NO. 244

MODELING THE SATURNIAN MAGNETOSPHERE FOR THE CASSINI MISSION

UNITED STATES NAVAL ACADEMY
ANNAPOLIS, MARYLAND

REPORT DOCUMENTATION PAGE

Form Approved
OMB No. 0704-0188

1. AGENCY USE ONLY (*Leave Blank*)	2. REPORT DATE	3. REPORT TYPE AND DATES COVERED
	1996	

4. TITLE AND SUBTITLE
Modeling the Saturnian magnetosphere for the Cassini Mission

5. FUNDING NUMBERS

6. AUTHOR(S)
Skubis, Mark D.

7. PERFORMING ORGANIZATION NAME(S) AND ADDRESS(ES)

8. PERFORMING ORGANIZATION REPORT NUMBER

9. SPONSORING/MONITORING AGENCY NAME(S) AND ADDRESS(ES)
United States Naval Academy
Annapolis, MD 21402

10. SPONSORING/MONITORING AGENCY REPORT NUMBER
USNA Trident Scholar report; no. 244 (1996)

11. SUPPLEMENTARY NOTES
Accepted by the U.S.N.A. Trident Scholar Committee

12a. DISTRIBUTION/AVAILABILITY STATEMENT
Approved for public release; distribution unlimited.

12b. DISTRIBUTION CODE
UL

13. ABSTRACT (*Maximum 200 words*)

This paper presents an advanced, three-dimensional model of the Saturnian magnetosphere. The magnetosphere field of Saturn is the sum of three contributions. The first two contributions, known as interior field sources, are the inherent planetary field and the field due to a co-rotating plasma ring around the planet. The third field contribution results from the interaction of the solar wind with the magnetopause (the magnetospheric boundary). This interaction induces currents on the magnetopause surface, which produces the additional field contribution. The Cassini Mission is a joint venture between the National Aeronautics and Space Administration and the European Space Agency, designed for study of the Saturn system. The mission planners require a magnetospheric model that will be valid at the time of the Cassini encounter (~June 2004). Previous models of the Saturn magnetospheric field either neglected the contribution from the solar wind or assumed a solar wind that approached the planet parallel to the plane of its magnetic equator. These models do not depict the solar wind orientation that Cassini will encounter at the beginning of its Tour, when the solar wind will approach from the maximum southern magnetic latitude. The model presented in this paper has been incorporated into Cassini Mission software to determine optimal orbiter configuration for the four-year tour.

14. SUBJECT TERMS
Saturn; Planetary magnetic fields; Magnetosphere; Magnetopause; Cassini

15. NUMBER OF PAGES
39

16. PRICE CODE

17. SECURITY CLASSIFICATION OF REPORT	18. SECURITY CLASSIFICATION OF THIS PAGE	19. SECURITY CLASSIFICATION OF ABSTRACT	20. LIMITATION OF ABSTRACT
UNCLASSIFIED	UNCLASSIFIED	UNCLASSIFIED	UL

U.S.N.A. --- Trident Scholar project report; no. 244 (1996)

MODELING THE SATURNIAN MAGNETOSPHERE FOR THE CASSINI MISSION

by

Midshipman Mark D. Skubis, Class of 1996
United States Naval Academy
Annapolis, Maryland

Mark D Skubis

Certification of Adviser Approval

Professor Irene M. Engle
Department of Physics

Irene M. Engle
3 May 1996

Acceptance for the Trident Scholar Committee

Professor Joyce E. Shade
Chair, Trident Scholar Committee

J. E. Shade
3 May 1996

USNA-1531-2

Abstract

This paper presents an advanced, three-dimensional model of the Saturnian magnetosphere. The magnetospheric field of Saturn is the sum of three contributions. The first two contributions, known as interior field sources, are the inherent planetary field and the field due to a co-rotating plasma ring around the planet. The third field contribution results from the interaction of the solar wind with the magnetopause (the magnetospheric boundary). This interaction induces currents on the magnetopause surface, which produces the additional field contribution. The Cassini Mission is a joint venture between the National Aeronautics and Space Administration and the European Space Agency, designed for study of the Saturn system. The mission planners require a magnetospheric model that will be valid at the time of the Cassini encounter (~ June 2004). Previous models of the Saturnian magnetospheric field either neglected the contribution from the solar wind or assumed a solar wind that approached the planet parallel to the plane of its magnetic equator. These models do not depict the solar wind orientation that Cassini will encounter at the beginning of its Tour, when the solar wind will approach from the maximum southern magnetic latitude. The model presented in this paper has been incorporated into Cassini Mission software to determine optimal orbiter configuration for the four-year tour.

Keywords: Saturn, Planetary Magnetic Fields, Magnetosphere, Magnetopause, Cassini

Table of Contents

I. Introduction

The Cassini Mission is a joint endeavor between the National Aeronautics and Space Administration (NASA), the European Space Agency (ESA), and the Italian Space Agency (ASI). The project is named in honor of Jean Dominique Cassini (1625-1712), an Italian-born, French astronomer who discovered the large division in Saturn's rings and four of the planet's moons. Scheduled for launch in October 1997 on board a Titan IV/Centaur rocket, the Cassini orbiter will journey to Saturn by way of gravity assists from Venus, Earth, and Jupiter. The spacecraft will be injected into Saturn orbit and begin its period of *in situ* observations in June 2004, whereupon the four-year (~ 60 orbit) data acquisition phase will begin [*Cassini Mission Plan*, 1995].

The goal of the Cassini Mission is to enhance understanding of the Saturnian system. To this end, the orbiter will focus on four areas of scientific investigation: the planet's atmosphere and rings, the planetary magnetosphere, the moon Titan, and the planet's icy satellites. Cassini will employ the most advanced sensor suite ever assembled, which will be used to create a comprehensive planetary database. The orbiter's instrumentation is crucial to mission success, and its effectiveness during its *in situ* period is highly dependent on the trajectory and orientation of the spacecraft.

The study of the Saturnian magnetosphere is the responsibility of the Cassini Mission's Magnetosphere and Plasma Science working group (MAPS). To insure optimal orbiter orientation for magnetospheric studies, MAPS requires a detailed, three-dimensional model of the planetary magnetospheric field. The magnetosphere is the region around the planet where its magnetic field is the dominant field. A well-defined boundary exists between the planetary magnetic field and interplanetary space. This boundary is referred to as the magnetopause.

Modeling the magnetosphere consists of predicting the location of the magnetopause and describing the magnetic field it encapsulates. Data collected by

Pioneer 11 (P11), Voyager 1 (V1), and Voyager 2 (V2) revealed that Saturn's magnetosphere is intermediate to those of Jupiter and Earth. Details about the global magnetosphere are limited, however, because the trajectories of the Pioneer and Voyager missions were limited to relatively constant magnetic latitudes and only one (V2) or two (P11, V1) crossings of the magnetic equator [*Connerney et al.*, 1981]. The detailed magnetospheric database that scientists need to construct an advanced, global magnetospheric model will be acquired by Cassini, which will collect data over a broad range of magnetic latitudes and longitudes.

MAPS incorporates magnetospheric models into the Jet Propulsion Laboratory's MAGPAC software package. This software allows the mission planning team to perform simulated flybys using different orbital trajectories and orientations. The results of these simulations will be used by the Tour planning team to determine how best to situate the orbiter for collection of magnetospheric data. After magnetospheric data collected by the orbiter has been transmitted to Earth and analyzed, the models used for Tour planning will serve as a point of origin for developing new models of the Saturnian magnetospheric field.

II. Background

The Saturnian magnetospheric field is the sum of three contributions. The first two contributions are referred to as the "interior sources" because they originate within the magnetosphere: they are the intrinsic planetary field and the field contribution from a toroidal plasma formation surrounding the planet. These sources, which are both axially and equatorially symmetric, have been deduced from Pioneer and Voyager observations. The third contribution to the planetary magnetospheric field is the result of the interaction of the solar wind with the magnetospheric field just inside the magnetopause. This

interaction induces currents on the magnetopause surface, thus producing a third magnetic field contribution.

Analysis of Pioneer and Voyager magnetometer data reveals that the intrinsic magnetic field of Saturn is well-represented by a planetary dipole field of moment ~ 0.21 $G \cdot R_S^3$ (1 R_S = 60,330 km). As is characteristic of a dipole field, it is nearly aligned (less than 1^o offset) with the planet's rotation axis [*Acuña and Ness*, 1980; *Ness et al.*, 1981,1982]. This alignment is unique to Saturn when compared to the Earth and Jupiter, and leads to the near-coincidence of the Saturnian rotational and magnetic planetary coordinate systems. The dipole field of Saturn is displayed in Figure 1 [*Maurice and Engle*, 1995].

Higher-order models of the intrinsic field have been developed [*Connerney et al.*, 1982; *Davis and Smith*, 1990], but they diverge from the dipole model only at distances close to the planet's surface. When treating the entire magnetospheric field, it is sufficient to represent the intrinsic planetary field as a dipole, $\mathbf{B}_{dipole}$. This field is likely the result of a dynamo effect, in which the metallic hydrogen zone (a region extending from 5000 km to 8000 km from the center of the planet) of the rapidly rotating planet produces a magnetic field contribution, d**B**, given by the Biot-Savart Law [*Zeilik*, 1991],

$$d\mathbf{B} = \frac{\mu_o}{4\pi} \frac{I\, d\mathbf{s} \times \hat{r}}{r^2} . \qquad (1)$$

I is the magnitude of the current, d**s** is a differential element indicating the direction of current flow, $\hat{r}$ is the unit vector in the direction from the source point to the field point, and r is the distance between the source point and the field point.

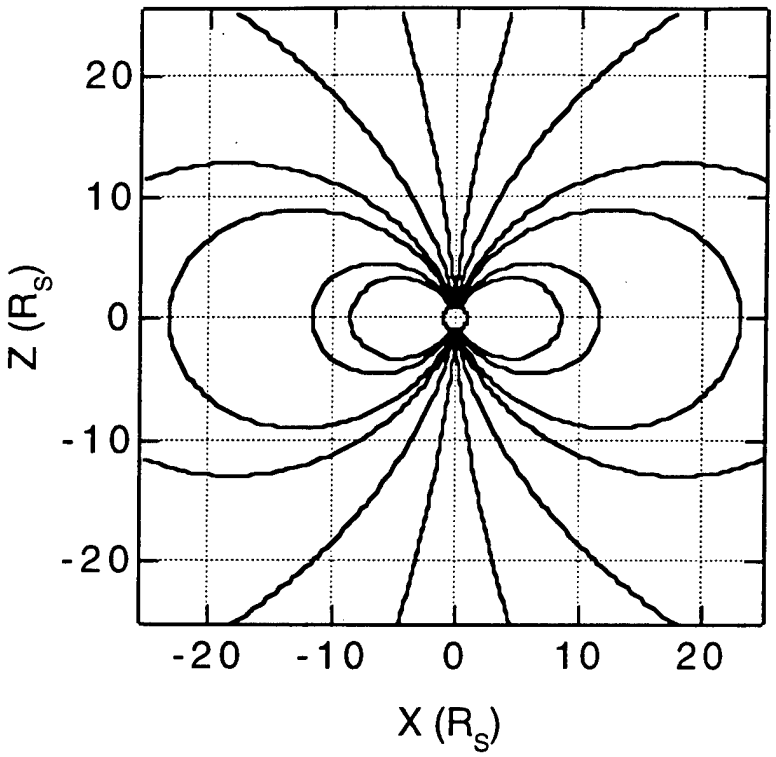

Figure 1. The dipole field of Saturn [*Maurice and Engle*, 1995]. The field lines lie in the noon/midnight (XZ) plane. Intensity of the field is a function of the density of the field lines. The X axis is the planetary magnetic equator and in the positive direction points to the Sun. The Z axis is the planetary magnetic axis, which is nearly coincident with the planetary rotation axis. The axes are measured in units of Saturnian radii (1 R_S = 60.330 km).

After further analysis of V1 data, *Connerney et al.* noted a departure from the dipole model beyond ~ 8 R_S on the day-side and outside ~ 5 R_S on the night-side of the planet. To account for this deviation they proposed an azimuthal current system whose magnetic field contribution, given by equation (1), was supported by experimental data [1981]. The V1 plasma experiment confirmed that the current system could be represented by a toroidal-shaped plasma region, whose cross section is a rectangle with inner and outer edges at 8 R_S and 15.5 R_S, respectively, and whose height is ~ 6 R_S [*Connerney et al.*, 1983].

Within the plasma "ring," the current density decreases radially as 1/r from a value of ~ 0.3×10^6 A/R_S^2 at the inner edge to ~ 0.15×10^6 A/R_S^2 at the outer edge of the formation. This ring, whose magnetic field contribution will henceforth be referred to as $\mathbf{B}_{ring}$, is similar in nature to the Jovian plasma disk [*Bode*, 1994]; however, it is about one order of magnitude smaller in terms of current density, contributing ~ 10 nT to the near-axis field. It is believed that the plasma is composed of light and heavy ions, probably hydrogen, oxygen, or nitrogen [*Bridge et al.*, 1981]. By superposition principles, $\mathbf{B}_{ring}$ and $\mathbf{B}_{dipole}$ add to yield the total magnetic field due to the internal magnetospheric sources. This field is displayed in Figure 2 [*Maurice and Engle*, 1995].

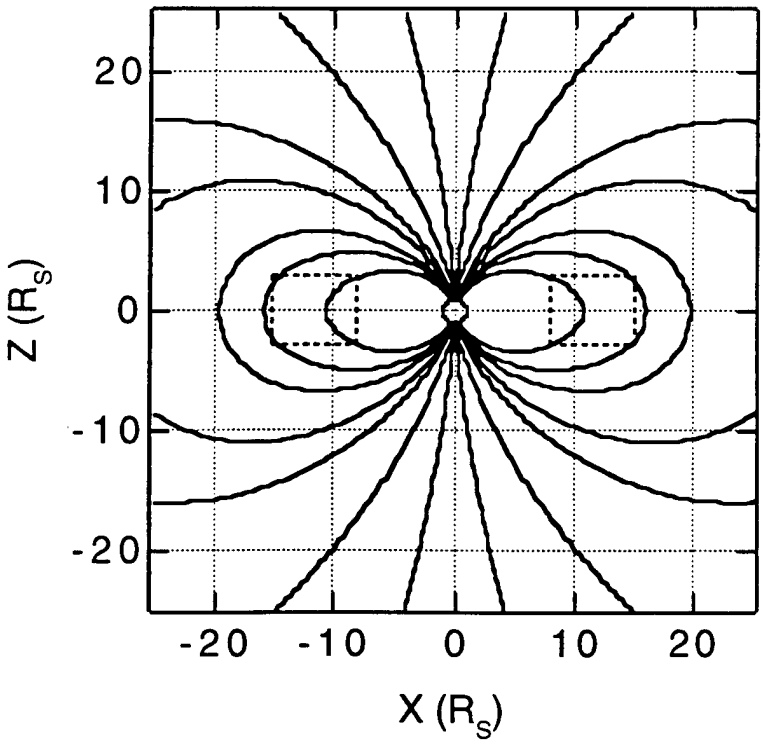

Figure 2. A view in the XZ plane of the sum of the dipole field and the field due to the plasma ring current ($\mathbf{B}_{dipole} + \mathbf{B}_{ring}$) [*Maurice and Engle*, 1995]. The regions bounded by dotted lines indicate where the plasma is contained. The field lines originate at the same latitudes as those in Figure 1.

The third contribution to the Saturnian magnetospheric field arises from the interaction of the solar wind with the magnetospheric field at the magnetopause. Solar wind is a supersonic particle flow emanating from the Sun that fills the interplanetary space of the solar system. It is composed of approximately equal numbers of electrons and protons, such that there is no net current produced by the wind. When this particle flow reaches the Saturnian magnetosphere, the charged particles of the flow are subjected to a magnetic force, **F**, given by

$$\mathbf{F} = q\mathbf{v} \times \mathbf{B}. \tag{2}$$

q is the charge on the particle, **v** is the velocity of the incoming particle, and **B** is the magnetic field that the particle encounters.

At moderate magnetic latitudes, this force redirects protons in a westward direction, while electrons are sent in an eastward path. The result is that a net current is formed on the magnetopause surface in the direction of proton deflection. The net current at each point on the surface of the magnetopause produces an additional magnetospheric field contribution, $\mathbf{B}_{MP}$, given by equation (1). This contribution vectorially adds with the interior field sources to arrive at the total magnetospheric field:

$$\mathbf{B} = \mathbf{B}_{dipole} + \mathbf{B}_{ring} + \mathbf{B}_{MP}. \tag{3}$$

III. Method

The interior sources of the planetary magnetosphere, $\mathbf{B}_{dipole} + \mathbf{B}_{ring}$, have an associated magnetic pressure. Likewise, the change in momentum of the solar wind particles as they enter the magnetosphere at the magnetopause exerts a Newtonian pressure. The balance between the magnetic pressure of the interior sources and the

incoming solar wind pressure permits the calculation of the three-dimensional magnetopause surface. The applicability of this condition is discussed in detail by *Beard* [1960] and *Mead and Beard* [1964].

The pressure balance equation at the magnetopause boundary is

$$2\rho_S V_S^2 \cos^2 \chi = \frac{B_T^2}{2\mu_o}. \tag{4}$$

χ is the angle between the incident solar wind and the normal to the magnetopause surface; B_T is the component of the net magnetic field at the boundary, and is approximately tangential to the magnetopause; and ρ_S and V_S are the mass density and the speed of the particle flow [*Maurice and Engle*, 1995]. The momentum conservation required by equation (4), in addition to accounting for all of the incoming solar wind particles, leads to the following working equation applicable at each point on the magnetopause surface:

$$\left| \hat{n}_s \times \mathbf{B} \right| \pm \hat{n}_s \cdot \hat{v} = 0. \tag{5}$$

The unit vector $\hat{n}_s$ is the normal to the magnetopause surface given in spherical polar coordinates by:

$$\hat{n}_s = K_n \left(\hat{r} - \frac{1}{r} \frac{\partial r}{\partial \theta} \hat{\theta} - \frac{1}{r \sin \theta} \frac{\partial r}{\partial \phi} \hat{\phi} \right) \tag{6}$$

where K_n is defined as:

$$K_n = \left[1 + \left(\frac{1}{r} \frac{\partial r}{\partial \theta} \right)^2 + \left(\frac{1}{r \sin \theta} \frac{\partial r}{\partial \phi} \right)^2 \right]^{-1/2}. \tag{7}$$

The unit vector $\hat{v}$ delineates the incoming solar wind direction. **B** is the total magnetic field vector, normalized to unity at the subsolar point, which is where the incoming solar wind is perpendicular to the magnetopause surface. In the first calculation of the magnetopause surface, **B** consists of only $\mathbf{B}_{dipole} + \mathbf{B}_{ring}$ because the contribution from the surface currents depends on that surface's curvature, which is not yet calculated [*Mead and Beard*, 1964].

Following construction of the trial surface, the first set of normalized magnetopause surface current elements can be computed according to:

$$\mathbf{J} = \hat{n}_S \times \mathbf{B}. \tag{8}$$

Substituting equations (6) and (7) into equation (8), one arrives at an alternate expression for **J**:

$$\mathbf{J} = \left(\frac{B_\theta}{r \sin\theta} \frac{\partial r}{\partial \phi} - \frac{B_\phi}{r} \frac{\partial r}{\partial \theta} \right) \hat{r} - \left(B_\phi + \frac{B_r}{r \sin\theta} \frac{\partial r}{\partial \phi} \right) \hat{\theta} + \left(B_\theta + \frac{B_r}{r} \frac{\partial r}{\partial \theta} \right) \hat{\phi}. \tag{9}$$

After these current elements have been computed for the entire magnetopause surface, they may be used to calculate a corresponding magnetic field contribution, $\mathbf{B}_{SC}$. This contribution is given by the Biot-Savart relationship in the following form:

$$\mathbf{B}_{n,\,SC} = \int \int \mathbf{J} \times \frac{(\mathbf{r} - \mathbf{r}')}{|\mathbf{r} - \mathbf{r}'|^3} \, dS'. \tag{10}$$

By substitution of equation (8) into equation (10), the following alternate expression is derived:

$$\mathbf{B}_{n,\,SC} = \int\int (\hat{n}_S \times \mathbf{B}_{n-1}) \times \frac{(\mathbf{r} - \mathbf{r}')}{|\mathbf{r} - \mathbf{r}'|^3}\, dS' \tag{11}$$

The procedure (5) - (11) is performed iteratively, incorporating new magnetopause surfaces and the corresponding current elements until the model becomes self-consistent. That is,

$$\mathbf{B}_{n,\,SC} = \mathbf{B}_{n-1,\,SC} \tag{12}$$

and, consequently,

$$\mathbf{B}_n = \mathbf{B}_{n-1}. \tag{13}$$

The currents on the magnetopause have a corresponding magnetic field contribution, $\mathbf{B}_{MP}$. At points inside the magnetosphere, the magnetic field may be represented as the gradient of a scalar magnetic potential, given in spherical polar coordinates by

$$\mathbf{B}_{MP}(r,\theta,\phi) = -\nabla\Phi_{MP}(r,\theta,\phi). \tag{14}$$

A possible expansion of $\Phi_{MP}(r,\theta,\phi)$ is

$$\Phi_{MP}(r,\theta,\phi) = \sum_{n=1}^{n_{max}} r^n \sum_{m=0}^{n} G_{nm}\, P_n^m(\cos\theta)\, [\cos(m\phi)]. \tag{15}$$

The coefficients G_{nm} are determined by using the calculated values of $\mathbf{B}_{MP}$ at points inside the magnetopause. This allows one to obtain the total magnetic field of the planet, given by

$$\mathbf{B} = \mathbf{B}_{dipole} + \mathbf{B}_{ring} + \mathbf{B}_{MP}. \quad (16)$$

IV. Existing models

Data collected by the magnetometers of P11, V1, and V2 has been used as the basis for the construction of several models of the Saturnian magnetospheric field. *Acuña et al.* [1980] present a field model based on analysis of P11 data [*Acuña and Ness*, 1979], and *Connerney et al.* [1981] present a model constructed from analysis of V1 data [*Ness et al.*, 1981]. Each of these models was based on two assumptions: a dipole representation of the inherent planetary field and the alignment of the planet's rotation and magnetic axes.

The planetary rotational and magnetic axes are not coincident with the magnetic axis offset by ~ 0.75° [*Ness et al.*, 1981]. The Zonal harmonic (Z_3) model, presented by *Connerney et al.* [1982], and the Saturn Pioneer Voyager (SPV) model, constructed by *Davis and Smith* [1990], attempt to account for the field contributions from the slight variation in alignment of the planetary rotational and magnetic axes. The variations between these models and the dipole-like models are minor, especially at larger distances from the planet. Additionally, these models do not account for the magnetic field contribution associated with the solar wind interaction at the magnetopause.

The P11, V1, and V2 encounters with the Saturnian magnetosphere were brief--on the order of hours--thereby limiting the potential to collect data. In addition to time constraints, magnetometer data collected by the probes was limited to small magnetic latitudes because of mission trajectories. Thus V2 crossed the magnetic equatorial plane

only once, while P11 and V1 each experienced only two crossings. The short *in situ* periods and the mission trajectories are the two factors that have limited the collection of Saturnian magnetospheric data. This, in turn, limits the aforementioned models to a small range of magnetic latitudes [*Connerney et al.*, 1981].

V. The *Maurice/Engle* idealized model

To extend the scope of knowledge of the Saturnian magnetosphere, *Maurice and Engle* constructed the first advanced three-dimensional model of the Saturnian magnetosphere [1995]. This model represents the Saturnian magnetospheric field based on the method outlined in Section III (although the method has been used to model the fields of Earth and Jupiter) [*Beard*, 1960; *Engle and Beard*, 1980].

The model constructed by *Maurice and Engle* (subsequently referred to as ME95) incorporated interior field sources due to the intrinsic planetary field and the ring current. Existing models attempted to represent these fields as well; however, this model differs from previous efforts because it took into account the contribution from the magnetopause surface currents. The result is that the physically reliable range of the model was extended to nearly all magnetic latitudes and longitudes within the Saturnian magnetosphere.

The Pioneer and Voyager missions encountered a large variability in the magnetic environment around Saturn. To account for this, ME95 modeled the magnetospheric field based on six parameters that describe the magnetosphere: one for the planetary field, four for the ring current, and one for the strength of the incoming solar wind. In their model, *Maurice and Engle* represented the planetary field by a dipole with moment of ~ $0.21\ G \cdot R_S^3$. The axially symmetric ring current proposed by *Connerney et al.* [1983] was incorporated, with $a = 8\ R_S$ and $b = 15.5\ R_S$. The average current strength was set

at I_o = 2.9 x 10^6 A/R_S, which is independent of its distance from the magnetic equator, $|z| \leq D = 3\ R_S$. The subsolar point was chosen to be $R_o = 20\ R_S$.

The parameters a, b, and D fix the dimensions of the toroidal plasma formation in Saturn's inner magnetosphere. With the corresponding current density I_o, the total current of the ring may be calculated and its contribution to the total magnetospheric field deduced. The subsolar point R_o is a parameter that represents the relative strength of the solar wind. Depending on the pressure of the wind, the location of the subsolar point will vary. The model presented by *Maurice and Engle* [1995] is displayed in Figure 3.

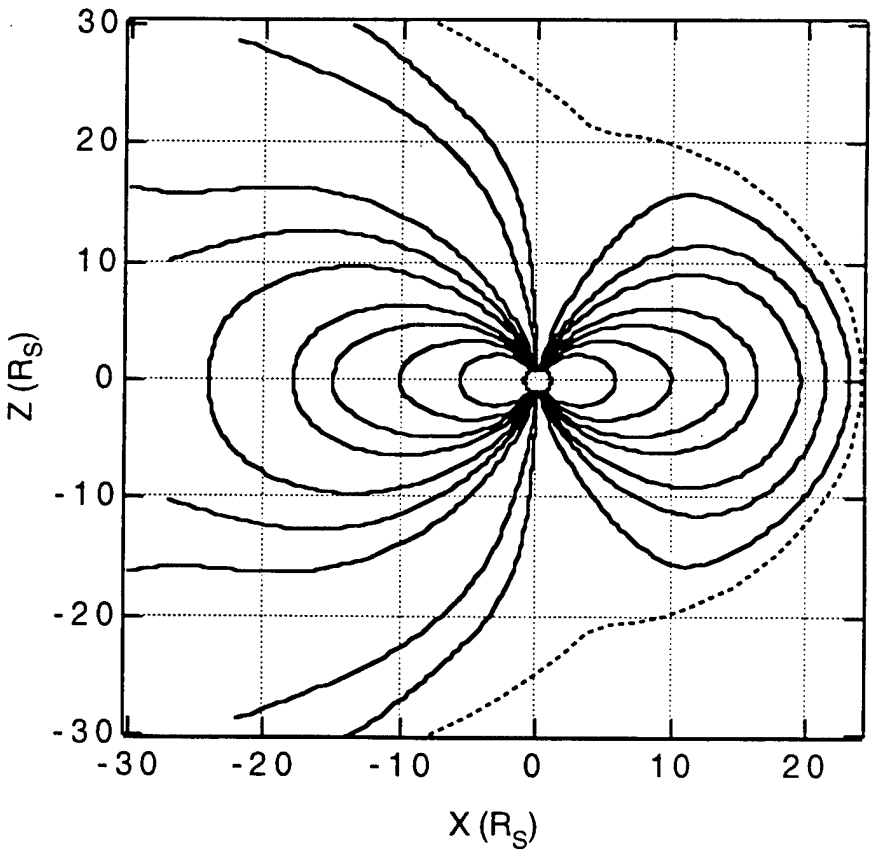

Figure 3. The noon/midnight view of the idealized magnetospheric model constructed by *Maurice and Engle* [1995]. The dotted line is the magnetopause surface. The solar wind is coming from the right, parallel to the X axis. This introduces symmetry about the X axis.

ME95 is referred to as an idealized model because of the direction of the incoming solar wind, which approaches parallel to the plane of the magnetic equator. This introduces a natural symmetry between the northern/southern hemispheres and the eastern/western hemispheres when calculating the magnetopause boundary. The calculation of the magnetopause surface is, therefore, reduced to one quarter of its total surface area. From that, the other three regions could be obtained immediately by applying symmetry considerations. While the solar wind approached in this manner at the time of the Pioneer and Voyager encounters with Saturn, this orientation will not be prevalent when Cassini arrives at the planet in June 2004.

VI. The solar wind variation

The orbital plane containing both Saturn and the Sun is referred to as the ecliptic plane. The rotation axis (axis about which the planet spins) of Saturn makes an angle of 26.7° with the normal to the ecliptic. This orientation is constant in space throughout the planet's orbit, leading to a cyclical variation of the rotation axis orientation with respect to the Sun over the course of a Saturn year (29.46 Earth years). The rings of Saturn lie in the planet's equatorial plane, to which the rotation axis is normal; therefore, the cyclical variation of the orientation of the rings with respect to the Sun corresponds to the variation of the rotation axis orientation during a Saturn year.

The change of Saturn's rotation axis orientation with respect to the Sun is analogous to the cause of seasons on Earth. Consider the first Saturnian season beginning when the rotation axis points toward the Sun. In this configuration, the rings of the planet will dip down when viewed from the Earth (or the Sun), making an angle of -26.7° with the ecliptic plane. A quarter cycle later, the axis points neither at the Sun nor away from the Sun. This neutral orientation means that the rings of the planet may be viewed edge-on from Earth. Next, the planet's rotation axis points away from the normal

to planet-sun line. During that era, the rings will appear tilted upward when viewed from the Earth. After the planet has proceeded through the last quarter of its orbit, the axis will once again be perpendicular to the sun-planet line and the rings may be viewed edge-on.

Based on Pioneer and Voyager data, it has been determined that the rotational and magnetic coordinate systems of Saturn are nearly coincidental, with the planetary magnetic axis offset from the planetary rotation axis by less than 1^{o}. As a result, the magnetic coordinate frame of the planet completes one full cycle with respect to the Sun in the same manner as does the rotational frame, namely, once every Saturnian year. This is a trait unique among planetary magnetospheres. The axis of Jupiter, for example, makes an angle of 10^{o} relative to the planetary rotation axis. Thus, the Jovian magnetosphere precesses about the planetary rotation axis on a daily (1 Jovian day = $9^{h}\ 55^{m}$) basis [*Bode*, 1994].

The configuration in which the rings of Saturn can be viewed edge-on occurs twice during a Saturnian year. This was the orientation during the Pioneer/Voyager epoch (~ 1980) and again in 1995, half an orbital cycle later. The ME95 model incorporates this orientation, which corresponded to data taken during the Pioneer/Voyager time frame. However, when Cassini arrives at the planet (~ June 2004), the planetary orientation will be such that the rotation axis is pointed away from the Sun (the rings are tilted up when viewed from the Earth). This presents a tour planning dilemma for the Cassini Mission.

The team planning Cassini's Tour requires a model of the magnetosphere of Saturn that can be anticipated at the beginning of the probe's *in situ* period. The changes in the Saturnian magnetosphere are related to the variation of the planet's position in orbit around the Sun. In order to anticipate this condition, one must anticipate the angle of incidence that the solar wind will have upon the Saturnian magnetopause, since it is a significant factor affecting the shape of the planetary magnetosphere.

While the solar wind does not emanate radially from the Sun, the distance that it travels before reaching Saturn insures that vectors representing the solar wind velocity will be parallel. Based on this fact, it is convenient to introduce the parameter λ. When the rings of Saturn are viewed edge-on from the Earth, the solar wind approaches parallel to the plane of the planetary magnetic equator. This corresponds to an angle of $\lambda = 0^{o}$. When the Cassini probe arrives at the planet, the rings will be near their maximum upward tilt as viewed from the Earth. Thus, the angle λ will take the same value as the angle between the plane of the rings and the ecliptic plane . As discussed previously, the solar wind will be incident at the largest possible value south of the magnetic equator, namely, at $\lambda = -26.7^{o}$.

VII. Constructing the $\lambda = -26.7^{o}$ model

This paper presents a magnetospheric model utilizing the condition $\lambda = -26.7^{o}$. The model, which anticipates the conditions at Saturn just prior to the arrival of Cassini, may be used by MAPS scientists at the Jet Propulsion Laboratory (JPL) in Cassini Mission simulation software, called MAGPAC. After MAPS converts the model into computer code, it is loaded into MAGPAC to perform simulated flybys of the planet. MAPS will determine the optimal orbiter configuration for magnetospheric data acquisition based on the MAGPAC simulations. Once this configuration is chosen, it will be considered with the requests of other mission scientists to fix the exact Tour of the spacecraft.

Construction of the $\lambda = -26.7^{o}$ model presented here began in a similar fashion to ME95. The magnetospheric environment of Saturn was again characterized by the six minimum parameters. The planetary field was represented as a dipole moment ~ 0.21 $G \cdot R_S^3$. The plasma current formation extended from $a = 8\ R_S$ to $b = 15.5\ R_S$, with a current density parameter of $2.9 \times 10^6\ A/R_S$. The height of the plasma ring above the

equatorial plane was $|z| \leq D = 2.8$ R_S. The subsolar point was chosen to be $R_o = 24$ R_S.

These parameters were fixed based on the parameters used in the ME95 model. Slight modifications were made, however, to scale the parameters to a different subsolar point. This was necessary because the subsolar point, while being indicative of the strength of the solar wind, is also representative of the value of the current circulating in the plasma ring. Based on the best fit to V1 data, the subsolar distance $R_o = 24$ R_S was chosen. This subsolar distance is consistent with the observed variations of the subsolar point, according to V1 observations.

Construction of the model first focused on building a trial magnetopause surface. Using a $5^o \times 5^o$ grid as a framework for numerical calculations, construction began using FORTRAN code on a Macintosh Quadra 800. First the noon meridian, which lies in the XZ plane in the planetary magnetic frame of reference, was calculated. Following this, the midnight meridian was computed. These meridia, because of the near-coincidence of the magnetic and rotation axes, inherently yielded a plausible surface meridia framework from which computation of the remainder of the surface was accomplished.

Construction of the ME95 model was required over only one quadrant of the magnetopause surface. The surface could then be extended to the other three quadrants by due to its four-fold symmetry. However, for the $\lambda = -26.7^o$ surface, the only symmetry present is that between the eastern and western hemispheres. As a result, calculations were performed over a surface area twice as large as the ME95 model. The breakdown of symmetry between the northern and southern hemispheres introduced programming challenges not encountered in the idealized situation.

While constructing the trial magnetopause surface, the computer calculated the difference between the $|\hat{n}_s \times \mathbf{B}|$ and the $|\hat{n}_s \cdot \hat{v}|$ terms of equation (5). The solution, which is a distance r from the planet, was chosen based on where this difference was

minimized. In attempting to find the surface point, the program first looked for a solution based on points in the neighboring region. If this failed, or no points had been calculated, the program set a maximum and minimum value for r. The lower limit was based on the calculation of the previous point, while the upper limit involved extrapolating a line perpendicular to the normal at the magnetopause surface of the previously calculated point.

The computer could be left to calculate the magnetopause surface on its own; however, the vast majority of its results would not be physically plausible. Scientists have attempted to automate the process, but due to the number of iterations required and the multitude of possible solutions involved in calculating a self-consistent magnetopause surface, however, these attempts have failed. The process requires the physical intuition of the physicist in order to choose numerical solutions that coincide with the current knowledge of planetary magnetospheres and the relatively vague boundary conditions, which introduce families of numerically valid but physically unacceptable solutions.

When the model was not near a state of self-consistency, solutions that yielded a more physically feasible surface were not selected by the program, which chooses the best numerical solution. To compensate for this, it was necessary to individually investigate solutions that posed physically unfeasible situations. This was done by inspecting the program outputs in an attempt to find local minima in the difference between the two terms of equation (5) that the computer may have overlooked. This was a crucial step in computing the first several iterations of the magnetopause surface.

VIII. Results of the $\lambda = -26.7^{o}$ model

Self-consistency of the $\lambda = -26.7^{o}$ model was achieved after ten iterations. The magnetopause surface that was calculated is displayed in Figure 4. The asymmetry effects of the solar wind are apparent when the $\lambda = -26.7^{o}$ magnetopause surface is

compared to the ideal surface of ME95. The incoming solar wind pressure tends to compress the region at the front of the magnetopause just below the day-side magnetic equatorial plane. Additionally, the solar wind pushes the magnetotail far above the magnetic equator of the planet on the dusk-side.

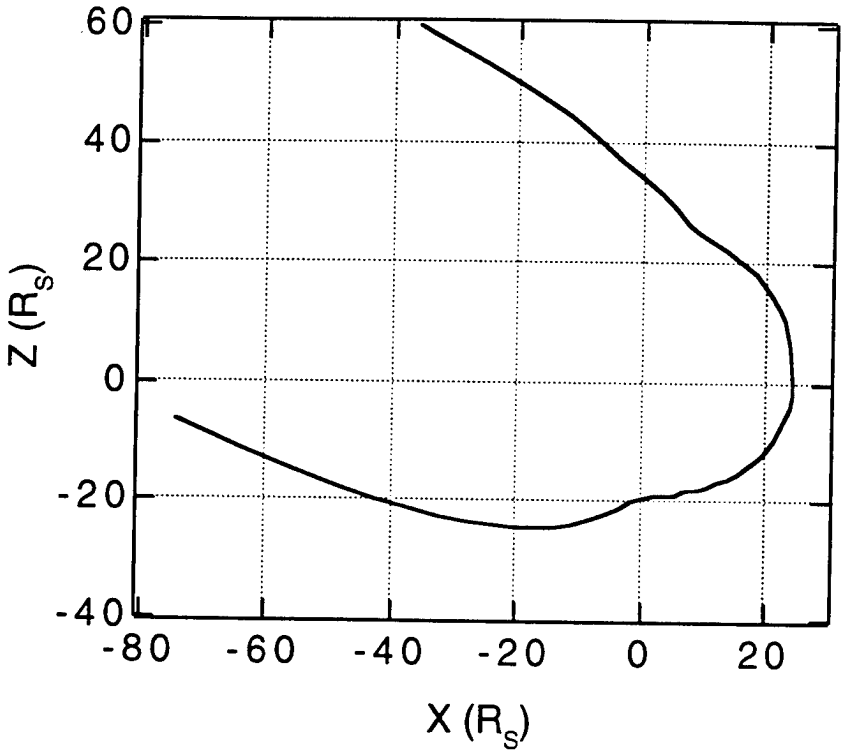

Figure 4. The magnetopause surface for the $\lambda = -26.7^{o}$ model.

After computing a self-consistent magnetopause surface, an expansion in associated Legendre functions yielded the coefficients G_{nm} that reproduce the planetary field lines according to equation (15), outlined in Section III. Appendix B lists the coefficients G_{nm} necessary to reproduce the magnetospheric field. This field is displayed in Figure 5.

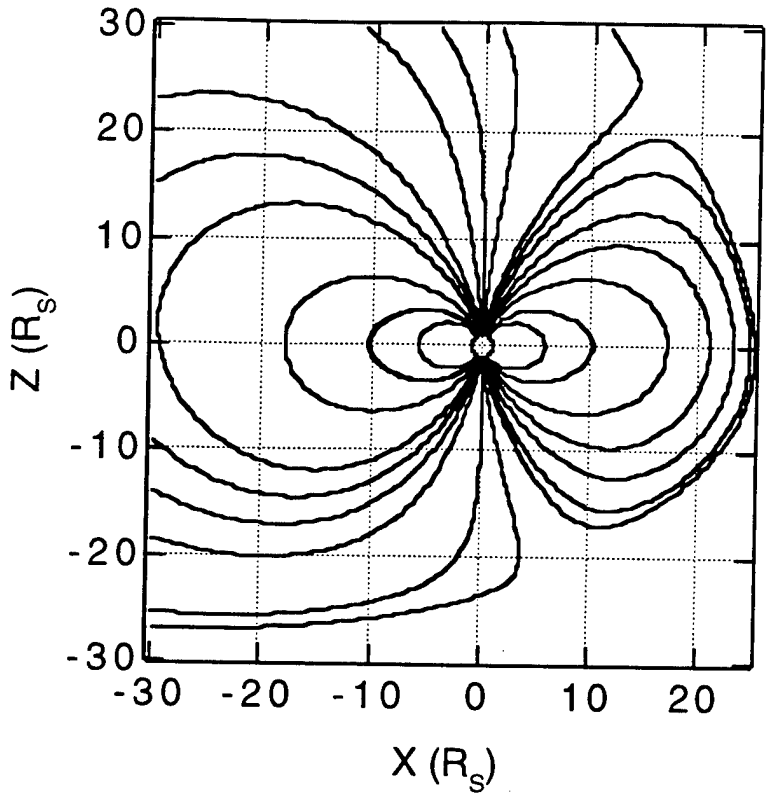

Figure 5. Field lines of the Saturnian magnetospheric field in the noon/midnight plane when λ = - 26.7°. The solar wind approaches from the right and makes an angle of - 26.7° with the X axis.

When compared to the ME95 idealized model, the effect of the solar wind asymmetry upon the shape of the magnetosphere is evident, particularly in the "cusp" regions of the field. The "cusp" is the region of the magnetosphere where the field lines cease to reconnect to the planet and, instead, sweep back to form the magnetotail. While the interior field near the magnetic equator is similar to that of the ME95 model, the cusp regions are quite different in terms of relative north and south field intensities and latitudes at which they occur. As the cusp regions are generally associated with planetary auroral phenomena, where charged particles spiral along magnetic field lines toward the planet surface, asymmetrical auroral phenomena should be anticipated in future observations.

Consideration of the field lines close to the planet's surface shows that the solar wind apparently both compresses the day-side field and pushes the night-side field lines upward. This compression may be seen in Figure 6. These field lines originate at the same magnetic latitude (S 80°) in the region of the southern cusp and are calculated around half of the planetary surface in 30° increments. The day-side field lines are clearly compressed by the solar wind, while the night-side lines appear relatively extended and pushed upward. The effect is most noticeable on the fourth field line from the right, which originates in the YZ plane. As the line travels further from the planet's surface it is pushed out of the YZ plane by the solar wind pressure.

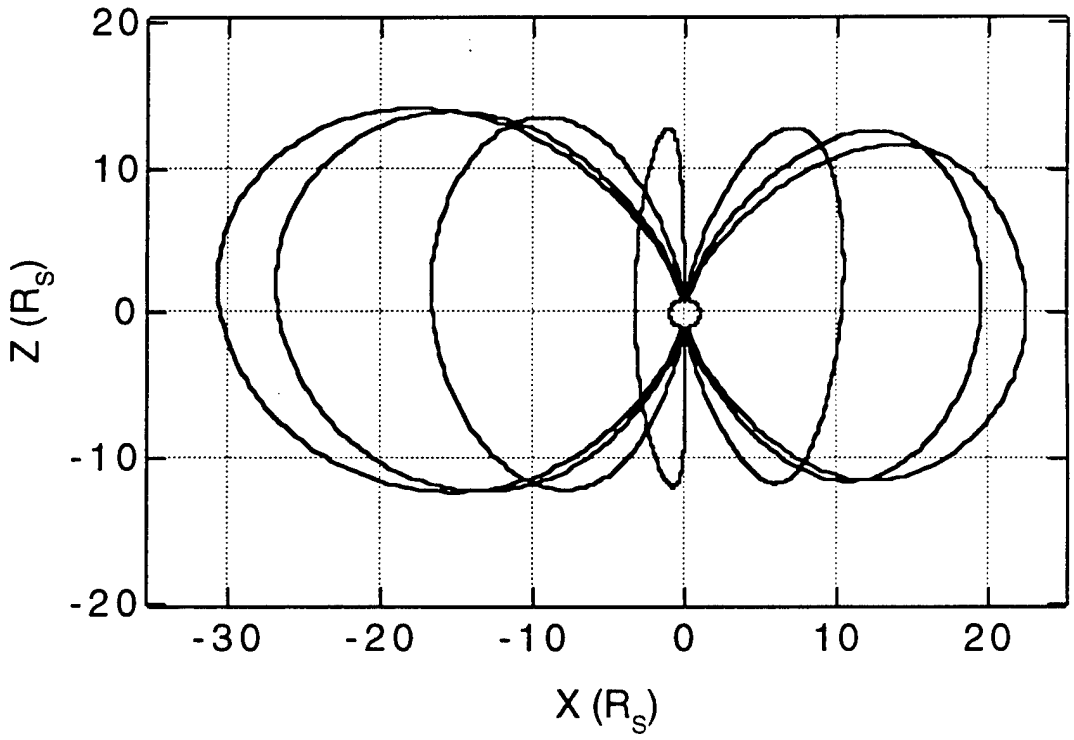

Figure 6. Field lines originating at a magnetic latitude of S 80°. The lines begin in the noon (positive X) plane, continuing in 30° increments to the midnight (negative X) plane.

IX. Validating the $\lambda = -26.7^{o}$ model

The *in situ* data that has been collected on the Saturnian magnetospheric field to date corresponds to measurements that were taken during the epoch of Pioneer and Voyager. Thus, because the solar wind was configured such that $\lambda \sim 0^{o}$, no direct observations are available to confirm the predictions of the $\lambda = -26.7^{o}$ model. There are, however, two ways that one may infer the accuracy of the model presented. One involves the successful application of the method used here to calculate the magnetospheric fields of Earth and Jupiter, while the other involves comparison of the magnetopause surfaces of Saturn as λ varies from -26.7^{o} to 0^{o}.

The method outlined in Section III has been applied to both Earth [*Beard*, 1960; *Mead and Beard*, 1964] and Jupiter [*Engle and Beard*, 1980; *Engle*, 1991]. In each case the field model was consistent with magnetospheric field data that has been collected. The Jovian model constructed using this method helped successfully explain the behavior of ionized effluvia of comet fragments from Shoemaker-Levy 9 prior to their impact with Jupiter in July 1994 [*Prangé et al.*, 1995].

Comparison of the ME95 model with V1 observations also lends validity to the model presented here. Through addition of the magnetopause surface current contribution to the planetary magnetic field, *Maurice and Engle* were able to greatly improve the fit between the observed data and the predicted values for the behavior of the magnetosphere in the outer region of the Saturnian magnetosphere ($17\ R_S < r < 24\ R_S$) [1995]. This region will be the focus of much of Cassini's magnetospheric studies. [*Cassini Mission Plan*, 1995].

Given the applicability of the ME95 model, a natural progression of magnetopause surfaces between the $\lambda = -26.7^{o}$ and the $\lambda = 0^{o}$ models would be a reasonable indication of the feasibility of the model presented in this paper. This was done, beginning with the self-consistent, $\lambda = -26.7^{o}$ magnetopause surface. Then the

value of λ was then varied in an ascending fashion to λ = - 20°, - 15°, - 10°, and - 5°. Trial magnetopause surfaces were constructed for each of these values of λ. The surfaces were not all calculated to the point of self-consistency; therefore, they are merely an attempt to observe the behavior of the magnetopause as the angle of incidence of the incoming solar wind increases from its minimum to the ideal case. The results may be seen in Figure 7.

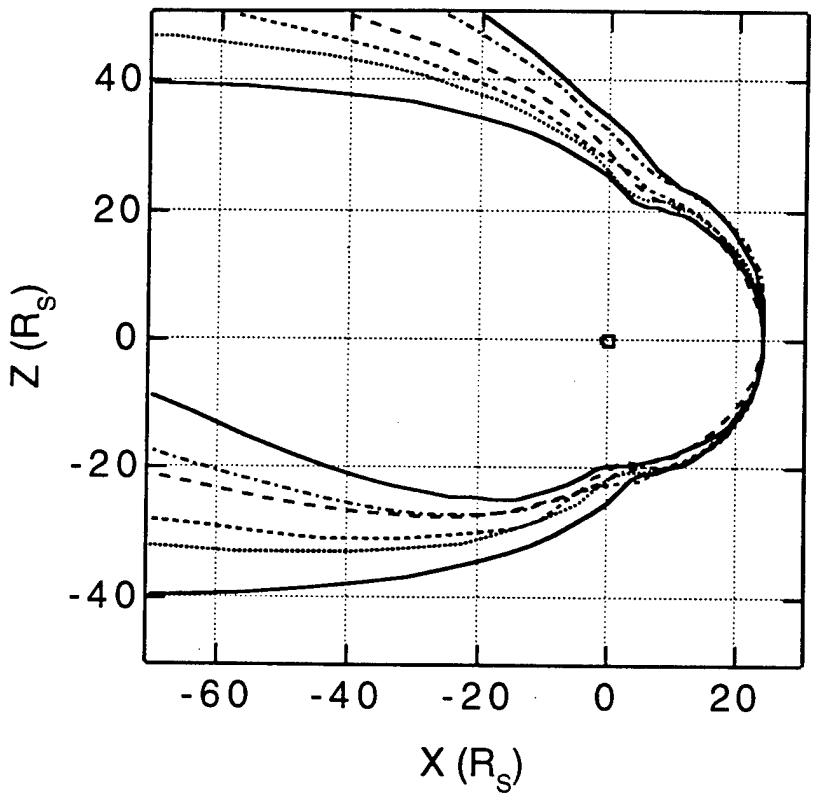

Figure 7. The magnetopause surface calculations for λ = - 26.7°, - 20°, - 15°, - 10°, - 5°, and 0°. For the λ = - 26.7° model to be physically feasible. the magnetopause surfaces must gradually transition between the extreme states. shown in the solid lines.

Figure 7 indicates a smooth transition between the extreme and ideal solar wind angles. As λ is varied to the ME95 condition, the magnetopause surfaces gradually shift between the ideal and the λ = - 26.7° configuration. This can best be seen by the varying

location of the cusp and the shift of the magnetotail toward its symmetrical configuration about the X axis. Each of the transition states presented is more "idealized" than the previous, an indication of the physical feasibility of the surfaces. Thus, it appears that the $\lambda = -26.7^{o}$ model is physically feasible.

X. Future applications

The model presented is the first in a series of steps to produce a time dependent model that will effectively predict the magnetospheric configuration at any point in the planet's orbit (that is, for any angle of incidence of the incoming solar wind). First, the development of self-consistent surfaces from the trial surfaces displayed in Figure 7 would yield field models and their associated expansion coefficients, G_{nm}. Once these expansion coefficients were known, they could be represented as functions of time that would successfully interpolate between values, predicting the coefficients of the various field models. This would eliminate the static nature of the model, making it instead a function of time capable of predicting the magnetospheric field for any angle λ based on the planet's position in its orbital cycle.

The tilted solar wind magnetopause surfaces displayed in Figure 7 are also being used to parameterize various configurations of the Saturnian magnetopause [*Maurice et al.*, 1996]. This is done by fitting ellipses to the surfaces in the YZ plane. These fits allow one to predict a value for r for any point on the magnetopause surface. This is significant because the method of the model presented limits knowledge of r to the nearest point on the $5^{o} \times 5^{o}$ grid that has been calculated. This functional representation of the magnetopause surface greatly extends our knowledge of the behavior of the magnetospheric boundary.

Advanced applications in the study of auroral phenomena, similar to those of Jupiter, are facilitated by the presentation of the $\lambda = -26.7^{o}$ magnetospheric model. As

previously stated, the interactions responsible for auroral phenomena are believed to be the result of charged particles trapped along field lines in the inner magnetosphere of the planet. In order to follow the regions in which charged particles may be accelerated by the field, it is imperative to know where on the surface the field lines originate and terminate. This permits the prediction of the location of auroral phenomena so that further research may take place.

XI. Conclusion

An ideal, three dimensional model of the Saturnian magnetosphere has been presented. Previous models either ignored the solar wind contribution to the magnetospheric field or examined the solar wind configuration that was prevalent during the Pioneer/Voyager epoch (1979-1981). The model presented differs from previous efforts in that it utilizes an incoming solar wind angle of $\lambda = -26.7^{o}$. This is the anticipated configuration of the solar wind at the time of injection of Cassini into orbit at Saturn (~ June 2004).

The model is required for use with the Cassini Tour planning team's MAGPAC software package, which allows the team to simulate flybys of the orbiter through its Tour utilizing various orientations. This will permit scientists to determine the optimal spacecraft configuration. The motivation for the optimum orientation is for the most efficient and productive collection of data that the orbiter can accomplish during its four-year tour. Currently, the model presented is being used by the Magnetosphere and Plasma Science working group of the Cassini Mission in tour simulation.

While the model is based on primarily theoretical calculations, the same process has been used successfully to model the magnetospheric fields of both the Earth and Jupiter. Additionally, trial magnetopause surfaces, obtained by varying the angle of incidence of the incoming solar wind from the maximum southern approach to the ideal

configuration of the ME95 model, implies that the model is physically feasible. This indicates that the model successfully models the magnetospheric field for the conditions that will exist just before the Cassini encounter.

Continuation of the work on the model presented will lead to magnetospheric models whose expansion coefficients can be replaced by functions in time that will successfully predict static field models. This will permit calculation of the field for any orientation of the incoming solar wind as a function of time. The model is also being used in work attempting to parameterize Saturnian magnetopause surfaces. This will allow the distance of the magnetopause to be calculated at any point over its surface, rather than the $5^{o} \times 5^{o}$ grid that is currently possible.

References

Acuña, Mario H., and Norman F. Ness, The Magnetic Field of Saturn: Pioneer Observations, *Science*, *207*, 444-446, 1980.

Acuña, M. H., N. F. Ness, and J. E. P. Connerney, The Magnetic Field of Saturn: Further Studies of the Pioneer 11 Observations, *J. Geophys. Res.*, *85*, 5675-5678, 1980.

Beard, David B., The Interaction of the Terrestrial Magnetic Field with the Solar Corpuscular Radiation, *J. Geophys. Res.*, *65*, 3559, 1960.

Behannon, K. W., J. E. P. Connerney, and N. F. Ness, Saturn's magnetic tail: structure and dynamics, *Nature*, *292*, 753-755, 1981.

Behannon, K. W., R. P. Lepping, and N. F. Ness, Structure and Dynamics of Saturn's Outer Magnetosphere and Boundary Regions, *J. Geophys. Res.*, *88*, 8791-8800, 1983.

Bode, Todd D., Modeling the Diurnally Precessing Jovian Magnetospheric Field, Trident Scholar project report no. 212, United States Naval Academy, Annapolis, Maryland, 1994.

Bridge, H. S., J. W. Belcher, A. J. Lazarus, S. Olbert, J. D. Sullivan, F. Bagenal, P. R. Gazis, R. E. Hartle, K. W. Ogilvie, J. D. Scudder, E. C. Sittler, A. Eviatar, G. L. Siscoe, C. K. Goertz, and V. M. Vasyliunas, Plasma Observations Near Saturn: Initial Results from Voyager 1, *Science*, *212*, 217-224, 1981.

Cassini Project, Mission Plan, *699-100, Rev. F* , Jet Propulsion Laboratory, Pasadena, California, 1995.

Connerney, J. E. P., M. H. Acuña, and N. F. Ness, Currents In Saturn's Magnetosphere, *J. Geophys. Res.*, *88*, 8779-8789, 1983.

Connerney, J. E. P., M. H. Acuña, and N. F. Ness, Saturn's ring current and inner magnetosphere, *Nature*, *292*, 724-726, 1981.

Connerney, J. E. P., N. F. Ness, and M. H. Acuña, Zonal harmonic model of Saturn's magnetic field from Voyager 1 and 2 observations, *Nature*, *298*, 44, 1982.

Davis, Leverett, Jr., and Edward J. Smith, A Model of Saturn's Magnetic Field Based on All Available Data, *J. Geophys. Res.*, *95*, 15,257-15,261, 1990.

Engle, Irene M., Idealized Voyager Jovian Magnetosphere Shape and Field, *J. Geophys. Res.*, *96*, 7793-7802, 1991.

Engle, Irene M., and David B. Beard, Idealized Jovian Magnetosphere Shape and Field, *J. Geophys. Res.*, *85*, 579-592, 1980.

Maurice, S., Irene M. Engle, M. Blanc, and M. Skubis, The Geometry of Saturn's Magnetopause Model, submitted for publication in *J. Geophys. Res.*

Maurice, S., and Irene M. Engle, Idealized Saturn magnetosphere shape and field, *J. Geophys. Res.*, *100*, 143-151, 1995.

Mead, Gilbert D. and David B. Beard, Shape of the Geomagnetic Field Solar Wind Boundary, *J. Geophys. Res.*, *69*, 1169, 1964.

Ness, Norman F., Mario H. Acuña, Ronald P. Lepping, John E. P. Connerney, Kenneth W. Behannon, Leonard F. Burlaga, and Fritz M. Neubauer, Magnetic Field Studies by Voyager 1: Preliminary Results at Saturn, *Science*, *212*, 211-217, 1981.

Ness, Norman F., Mario H. Acuña, Kenneth W. Behannon, Leonard F. Burlaga, John E. P. Connerney, Ronald P. Lepping, and Fritz M. Neubauer, Magnetic Field Studies by Voyager 2: Preliminary Results at Saturn, *Science*, *215*, 558-563, 1982.

Prangé, R., I. Engle, J. T. Clarke, M. Dunlop, G. E. Ballester, W. H. Ip. S. Maurice, and J. Trauger, Auroral Signature of Comet SL9 in the Jovian Magnetosphere, *Science*, *267*, 1317-1319, 1995.

Sittler, E. C., Jr., K. W. Ogilvie, and J. D. Scudder, Survey of Low-Energy Plasma Electrons in Saturn's Magnetosphere: Voyagers 1 and 2, *J. Geophys. Res.*, *88*, 8847-8870, 1983.

Slavin, J. A., E. J. Smith, P. R. Gazis, and J. D. Mihalov, A Pioneer-Voyager Study of the Solar Wind Interaction With Saturn, *Geophys. Res. Lett.*, *10*, 9-12, 1983.

Smith, Edward J., Leverett Davis Jr., Douglas E. Jones, Paul J. Coleman Jr., David S. Colburn, Palmer Dyal, and Charles P. Sonett, Saturn's Magnetosphere and Its Interaction With the Solar Wind, *J. Geophys. Res.*, *85*, 5655-5674, 1980.

Zeilik, Michael, *Astronomy: the Evolving Universe*, John Wiley & Sons, p. 215, 1991.

APPENDIX A: FREQUENTLY USED SYMBOLS

Symbols used in the text are listed below, in order of appearance.

Symbol	Definition
G	gauss; unit of measure of magnetic field; 1 T = 10^4 G
R_S	Saturnian radius; ~ 60,330 km
$\mathbf{B}_{dipole}$	magnetic field contribution from planetary dipole field
$d\mathbf{B}$	differential magnetic field element
μ_o	permeability of free space; $4\pi \times 10^{-7}$ N/A^2
I	current magnitude
$d\mathbf{s}$	differential directional current element
$\hat{r}$	unit vector in direction from source point to field point
r	distance from source point to field point
$\mathbf{B}_{ring}$	magnetic field contribution from co-rotating plasma ring
F	force
q	charge
v	velocity
$\mathbf{B}_{MP}$	magnetic field of the magnetopause
ρ_s	mass density of solar wind particles
V_s	speed of solar wind particles
χ	angle between solar wind and normal to the magnetopause
B_T	tangential component of magnetic field at the magnetopause
$\hat{n}_s$	unit vector normal to the magnetopause
$\hat{v}$	unit vector in direction of solar wind

Symbol	Definition
$\mathbf{J}$	current density
$\mathbf{B}_{SC}$	magnetic field contribution from magnetopause surface currents
$\mathbf{B}_n$	n^{th} iteration of the magnetic field
$\mathbf{r}$	distance vector from origin to source point
$\mathbf{r}'$	distance vector from origin to field point
dS'	differential distance element
∇	gradient
Φ_{MP}	scalar potential corresponding to $\mathbf{B}_{MP}$
G_{nm}	expansion coefficients for the total magnetospheric field
$P_n^m(\cos\theta)$	Associated Legendre polynomials
a	inner radius of plasma region, as measured from planet's center
b	outer radius of plasma region, as measured from planet's center
D	height of plasma region above equatorial plane
I_o	current density parameter
R_o	subsolar point, as measured from planet's center

APPENDIX B: THE COEFFICIENTS G_{nm}

The expansion coefficients G_{nm} used in equation (15) to produce the magnetospheric field line models for the conditions $\lambda = 0^o$ [*Maurice and Engle*, 1995] and $\lambda = -26.7^o$.

G (n,m)	$\lambda = 0^o$	$\lambda = -26.7^o$
G (1,0)	6.58E-01	6.61E-01
G (1,1)	0	-5.34E-02
G (2,0)	0	-2.10E-01
G (2,1)	3.34E-01	2.74E-01
G (2,2)	0	-7.86E-03
G (3,0)	2.23E-02	7.75E-02
G (3,1)	0	-8.99E-02
G (3,2)	6.85E-02	6.27E-02
G (3,3)	0	-7.03E-03
G (4,0)	0	-4.26E-02
G (4,1)	7.19E-02	6.67E-02
G (4,2)	0	-1.22E-02
G (4,3)	8.21E-03	1.89E-02
G (4,4)	0	-7.28E-03
G (5,0)	-8.70E-03	3.65E-03
G (5,1)	0	-3.89E-02
G (5,2)	3.63E-02	2.34E-02
G (5,3)	0	1.18E-02
G (5,4)	-2.26E-05	1.29E-02
G (5,5)	0	-3.97E-03

G (n,m)	$\lambda = 0^o$	$\lambda = -26.7^o$
G (6,0)	0	2.77E-03
G (6,1)	1.82E-02	6.31E-03
G (6,2)	0	-1.89E-02
G (6,3)	1.35E-02	1.41E-03
G (6,4)	0	8.56E-03
G (6,5)	-5.54E-05	8.79E-03
G (6,6)	0	-9.19E-04
G (7,0)	-1.26E-02	7.21E-04
G (7,1)	0	8.23E-04
G (7,2)	1.59E-02	4.12E-03
G (7,3)	0	-4.93E-03
G (7,4)	5.03E-03	-1.19E-03
G (7,5)	0	2.38E-03
G (7,6)	-3.39E-04	3.59E-03
G (7,7)	0	-2.89E-04
G (8,0)	0	-1.94E-04
G (8,1)	-5.19E-05	1.63E-06
G (8,2)	0	2.14E-06
G (8,3)	5.48E-03	8.79E-04
G (8,4)	0	-4.13E-04
G (8,5)	1.99E-03	2.42E-05
G (8,6)	0	5.03E-04

G (n,m)	$\lambda = 0^o$	$\lambda = -26.7^o$
G (8,7)	-1.26E-04	8.58E-04
G (8,8)	0	-3.10E-04
G (9,0)	-9.25E-03	4.90E-05
G (9,1)	0	1.96E-06
G (9,2)	1.34E-04	-5.84E-06
G (9,3)	0	2.57E-05
G (9,4)	3.06E-03	-9.87E-05
G (9,5)	0	-5.61E-05
G (9,6)	9.26E-04	1.02E-04
G (9,7)	0	1.19E-04
G (9,8)	-1.19E-04	1.22E-04
G (9,9)	0	-1.74E-04
G (10,0)	0	-5.29E-07
G (10,1)	-2.01E-04	5.69E-07
G (10,2)	0	7.31E-06
G (10,3)	7.42E-04	3.14E-06
G (10,4)	0	1.05E-05
G (10,5)	-2.98E-04	-2.88E-05
G (10,6)	0	-1.82E-05
G (10,7)	3.62E-04	-1.95E-06
G (10,8)	0	7.74E-06
G (10,9)	2.58E-07	-5.40E-08

G (n,m)	$\lambda = 0^o$	$\lambda = -26.7^o$
G (10,10)	0	-1.39E-07